

Measuring Higgs  $\mathcal{CP}$  and couplings with hadronic event shapesChristoph Englert,<sup>1,\*</sup> Michael Spannowsky,<sup>1,†</sup> and Michihisa Takeuchi<sup>2,‡</sup><sup>1</sup>*Institute for Particle Physics Phenomenology, Department of Physics,  
Durham University, DH1 3LE, United Kingdom*<sup>2</sup>*Institute for Theoretical Physics, Heidelberg University, 69120 Heidelberg, Germany*

Experimental falsification or validation of the Standard Model of Particle Physics involves the measurement of the  $\mathcal{CP}$  quantum number and couplings of the Higgs boson. Both ATLAS and CMS have reported an SM Higgs-like excess around  $m_H = 125$  GeV. In this mass range the  $\mathcal{CP}$  properties of the Higgs boson can be extracted from an analysis of the azimuthal angle distribution of the two jets in  $pp \rightarrow Hjj$  events. This channel is also important to measure the couplings of the Higgs boson to electroweak gauge bosons and fermions, hereby establishing the exceptional role of the Higgs boson in the Standard Model. Instead of exploiting the jet angular correlation, we show that hadronic event shapes exhibit substantial discriminative power to separate a  $\mathcal{CP}$  even from a  $\mathcal{CP}$  odd Higgs. Some event shapes even show an increased sensitivity to the Higgs  $\mathcal{CP}$  compared to the azimuthal angle correlation. Constraining the Higgs couplings via a separation of the weak boson fusion and the gluon fusion Higgs production modes can be achieved applying similar strategies.

## I. INTRODUCTION

Experimental searches for the Standard Model (SM) Higgs boson [1] performed by ATLAS and CMS [2, 3], based on a combination of luminosities of up to about  $2.3 \text{ fb}^{-1}$  per experiment [4], exclude a SM-like Higgs boson between 141 GeV and 476 GeV at 95% confidence level (CL). By the end of December 2011 both ATLAS and CMS updated the Higgs search using the entirely available data set, refining the analyses with integrated luminosities of up to  $5 \text{ fb}^{-1}$  [5–7], depending on the channel. This allowed to raise the lower Higgs mass bound from LEP2 of 114.4 GeV [8] to 117.5 by ATLAS. By now the Higgs is excluded at 95% CL from 129 (127.5) GeV to 539 (600) GeV by ATLAS (CMS). Strong bounds as low as fractions  $\sigma/\sigma^{\text{SM}} \lesssim 0.3$  for some Higgs mass ranges have been established. However, both ATLAS and CMS have also presented tantalizing hints of a  $m_H \simeq 125$  GeV Higgs boson, with local significances of  $2.5\sigma$  and  $2.8\sigma$  respectively. Together with the recently reported  $2.2\sigma$  excess from updated searches by the Tevatron experiment [9], the hints for a light Higgs around this particular mass seem to consolidate and various new physics interpretations of the excess have already been considered in Refs. [10–13]. While a  $5\sigma$  discovery could be achieved in the near future, all properties of this newly discovered state other than its mass are going to be rather vaguely known due to limited statistics (see *e.g.* Ref. [14]). The question of whether we indeed observe the SM Higgs can only be addressed with higher luminosity and larger center of mass energy.

A crucial step towards a further validation of the SM Higgs sector after the discovery of the resonance is the determination of its spin, its  $\mathcal{CP}$  quantum number and its

couplings to fermions and gauge bosons. In fact, because the observed resonance seems to decay into photons, the Landau-Yang theorem [15, 16] excludes the resonance to be a spin-1 particle\*. This leaves the measurement of the resonance's couplings and  $\mathcal{CP}$  the theoretically most interesting ones.

In the SM, the Higgs boson is the (indispensable) remnant of the  $SU(2)$ -doublet Higgs field after spontaneous symmetry breaking. To establish that a single Higgs field is responsible for the generation of fermion and electroweak-gauge-boson masses, eventually, the couplings of the Higgs boson to all SM particles have to be measured accurately. The major production processes of a light Higgs boson at the LHC are the gluon fusion (GF) [17] and the weak boson fusion (WBF) [18, 19] channels. The GF channel is induced by heavy fermion loops connecting the initial state gluons with the Higgs boson, while the WBF channel relies on the large Higgs coupling to electroweak gauge bosons to produce the Higgs in association with two tagging jets. When extracting its couplings from data, the production of the Higgs boson and its decay cannot be treated independently [20]: The observed number of Higgs bosons depends on the coupling responsible for Higgs boson production  $g_p$  and the size of the coupling which dials the Higgs decay into a specific final state  $g_d$ , so schematically we observe

$$\sigma_p \cdot \text{BR}_d \sim g_p^2 \frac{g_d^2}{\Gamma_H}. \quad (1)$$

Note that even if  $g_p = g_d$  the total width of the Higgs boson  $\Gamma_H$  is sensitive to all Higgs couplings, but a direct measurement of  $\Gamma_H$  is not possible at hadron colliders due to systematics.

A channel, which is phenomenologically well-suited to study longitudinal gauge boson scattering [21] and

\*Electronic address: christoph.englert@durham.ac.uk

†Electronic address: michael.spannowsky@durham.ac.uk

‡Electronic address: m.takeuchi@thphys.uni-heidelberg.de

\*However, spin-0 or higher spin states are not excluded and an experimental validation is desirable.

Higgs couplings to electroweak gauge bosons is  $pp \rightarrow \text{Higgs}+2 \text{ jets}$  (with subsequent Higgs decay). In this channel, it is particularly difficult to separate gluon fusion from the weak boson fusion contribution since both production modes exhibit similar cross sections for typical event selection cuts [22, 23]. Because  $g_p \simeq g_{p,\text{GF}} + g_{p,\text{WBF}}$  in Eq. (1), the uncertainties of different Higgs couplings obtained from experimental analyses in this channel are correlated and the extraction of the individual couplings becomes challenging [20].

For a 125 GeV SM Higgs-like resonance, we have to face the phenomenological impediment that standard  $\mathcal{CP}$  analyses [24] of the so-called gold-plated final state  $H \rightarrow ZZ \rightarrow 4\ell$  [25], which employ strategies closely related to the one proposed by Cabibbo and Maksymowicz in the context of kaon physics [26–28] are statistically limited even at  $\sqrt{s} = 14$  TeV. Instead, the jet-azimuthal angle correlation in Higgs+2 jets events with  $H \rightarrow \tau^+\tau^-$  has been put forward as an excellent probe of the  $\mathcal{CP}$  nature of the Higgs boson in series of seminal papers [19, 29, 30]. Since then a lot of effort has been devoted to theoretical and phenomenological refinements of this important channel. These range from precise (fixed higher order QCD) predictions of the contributing signal and background processes [23, 31–34] over resummation [35, 36] to the generalization to the other important final state for a light Higgs,  $H \rightarrow WW$  [37]. Only recently, the  $pp \rightarrow Hjj \rightarrow \tau^+\tau^-jj$  channel was studied for the first time at the LHC to derive bounds on the SM Higgs boson production cross section [38]. This impressively demonstrates that experimental systematics in this important channel are well under control, already now with early data.

The azimuthal angle correlation of the tagging jets as a  $\mathcal{CP}$ -discriminative observable can be rephrased in the following way: Once the Higgs is identified, the hadronic energy flow of the event depends on the  $\mathcal{CP}$  quantum number of the produced Higgs. The correlation of in the azimuthal angle should also be reflected in the global structure of softer tracks, which do not give rise to resolved jets. It is precisely the hadronic energy flow which is captured by event shape observables in theoretically favorable way [39], turning them into natural candidates to be considered among the  $\mathcal{CP}$ -discriminative observables in the context of  $\mathcal{CP}$  analyses. From a perturbative QCD point of view, the phenomenology of event shapes [39] possesses a number of advantages over “traditional” jet-based observables. In particular, provided that the observables are “continuously global” [40, 41], they can be resummed to NLL beyond the leading color approximation. Therefore, event shapes offer a good theoretical handle to potentially reduce perturbative uncertainties.

We organize this work in the following way: Sec. II briefly reviews the hadronic event shape and the  $\Delta\Phi_{jj}$  observables, which we consider in the course of this paper. We outline the details of our analysis in Sec. III. We discuss the sensitivity of event shapes in  $\mathcal{CP}$  analyses of Higgs+2 jets events in Sec. IV, where we also investigate

the possibility to distinguish WBF from GF invoking the same observables. Before we give our conclusions and an outlook in Sec. V, we briefly comment on pile-up issues that can arise in the suggested analysis in Sec. IV D.

## II. EVENT SHAPE OBSERVABLES AND $\Delta\Phi_{jj}$

Event shapes quantify geometrical properties of the final state’s energy flow<sup>†</sup>. An event shape, which is well-known from QCD measurements performed during the LEP era [42, 43] is **thrust**  $T$  [44]. In its formulation in the beam-transverse plane this observable is also meaningful at hadron colliders,

$$T_{\perp,g} = \max_{\mathbf{n}_T} \frac{\sum_i |\mathbf{p}_{\perp,i} \cdot \mathbf{n}_T|}{\sum_i |\mathbf{p}_{\perp,i}|}. \quad (2)$$

The subscript  $g$  indicates that this is a continuously global observable [41]. The three vectors  $\mathbf{p}_{\perp,i}$  are the beam-transverse momentum components of the particle  $i$  (*i.e.* a ATLAS topocluster or a CMS particle flow object), while the sum runs over all detected particles (typically in  $|\eta_i| \leq 4.5$ ). In a nutshell,  $T_{\perp,g}$  measures how circularly symmetric ( $T_{\perp,g} = 0.5$ ) or how pencil-like ( $T_{\perp,g} \rightarrow 1$ ) an event appears to be in the transverse plane. The vector  $\mathbf{n}_T$  in the transverse plane that maximizes Eq. (2) is called the transverse thrust axis.

Another event shape, familiar from  $e^+e^-$  physics, which can be straightforwardly adapted to hadron collider physics analogous to Eq. (2) is **thrust minor**

$$T_{m,g} = \frac{\sum_i |\mathbf{p}_{\perp,i} \times \mathbf{n}_T|}{\sum_i |\mathbf{p}_{\perp,i}|}. \quad (3)$$

$T_{m,g}$  provides a measure of the energy flow in the transverse plane perpendicular to  $\mathbf{n}_T$ .

As already mentioned, the tagging jet azimuthal angle correlation is a  $\mathcal{CP}$ -discriminative observable in Higgs+2 jets production.  $\Delta\Phi_{jj}$  can be defined as the angle between all jets  $j$  with rapidity smaller and all jets with rapidity larger than the reconstructed Higgs [23, 35]

$$p_{<}^{\mu} = \sum_{j \in \{\text{jets: } y_j < y_h\}} p_j^{\mu}, \quad p_{>}^{\mu} = \sum_{j \in \{\text{jets: } y_j > y_h\}} p_j^{\mu} \quad (4)$$

$$\Delta\Phi_{jj} = \phi(p_{>}) - \phi(p_{<}).$$

The special role played by the tagging jets in  $\Delta\Phi_{jj}$  is best reflected in the **cone thrust minor** event shape. Its definition is similar to Eq. (3), but only particles which fall into the vicinity of two reconstructed kT jets [45] with some resolution  $D$  (we will assume  $D = 0.4$  in the following) are considered in the sum.

<sup>†</sup>The phenomenology and resummation of a large class of event shape observables at hadron colliders has recently been discussed in Refs. [39, 41].

Typical selection cuts which are used to suppress the contributing backgrounds often involve the requirement that the tagging jets fall into opposite hemispheres  $y_{j_1} \cdot y_{j_2} < 0$  while the Higgs is produced in the central part of the detector. Observing  $\mathcal{CP}$  sensitivity in the  $\Delta\Phi_{jj}$  distribution suggests that broadening observables [46] also carry information about the Higgs  $\mathcal{CP}$ . We divide the event up according to the transverse thrust axis

$$\begin{aligned} \text{region } D: & \quad \mathbf{p}_{\perp,i} \cdot \mathbf{n}_T > 0 \\ \text{region } U: & \quad \mathbf{p}_{\perp,i} \cdot \mathbf{n}_T < 0 \end{aligned} \quad (5a)$$

and compute the weighted pseudorapidity and azimuthal angle

$$\eta_X = \frac{\sum_i |\mathbf{q}_{\perp,i}| \eta_i}{\sum_i |\mathbf{q}_{\perp,i}|}, \quad \phi_X = \frac{\sum_i |\mathbf{q}_{\perp,i}| \phi_i}{\sum_i |\mathbf{q}_{\perp,i}|}, \quad X = U, D. \quad (5b)$$

$\eta_i$  and  $\phi_i$  are the pseudorapidity and azimuthal angle of the vector  $i$  respectively. From these we can compute the broadenings of the  $U$  and  $D$  regions

$$B_X = \frac{1}{Q_T} \sum_{i \in X} |\mathbf{q}_{\perp,i}| \sqrt{(\eta_i - \eta_X)^2 + (\phi_i - \phi_X)^2}, \quad X = U, D \quad (5c)$$

where

$$Q_T = \sum_i |\mathbf{q}_{\perp,i}|. \quad (5d)$$

The **central total broadening** and **wide broadening** are defined as [39, 42]

$$\begin{aligned} \text{central total broadening: } & B_T = B_U + B_D, \\ \text{wide broadening: } & B_W = \max\{B_U, B_D\}. \end{aligned} \quad (5e)$$

The observables Eqs. (2), (3), and (5) do not exhaust the list of existing event shapes by far but they are sufficient for the purpose of this work.

### III. ELEMENTS OF THE ANALYSIS

#### A. Event generation

##### Signal

Event shapes are known to be well-reproduced by matched shower Monte Carlo programs [39]. Therefore, we generate MLM-matched [47] scalar  $Hjj$  and pseudoscalar  $Ajj$  samples with MADEVENT v4 [48] in the effective  $ggH$  and  $ggA$  coupling approximation and shower the events with PYTHIA [49]. We normalize the event samples to the NLO QCD cross section, which we obtain by running MCFM [50] for the gluon fusion contributions,

and VBFNLO [51] for the weak boson fusion contributions. The interference effects are known to be negligible for weak boson fusion cuts [52]. Note that there is no WBF contribution for the  $\mathcal{CP}$  odd scalar  $A$ . Nonetheless it is customary to analyze  $Ajj$  and  $Hjj$  samples for identically chosen normalizations to study the prospects of discriminating ‘‘Higgs-lookalike’’ scenarios [53, 54].

We find a total Higgs-inclusive normalization (considering  $\sqrt{s} = 14$  TeV) of  $\sigma_H = 3.2$  pb. For the  $\mathcal{CP}$  odd scalar we use  $\sigma_A = 2.1$  pb which adopts the NLO QCD gluon fusion  $K$  factor of  $\mathcal{CP}$  even Higgs production. In Sec. IV B we also discuss our results for identical normalizations, which focuses on the discriminating power of different shapes instead of a combination of shapes and different total cross sections. The ditau branching ratio to light opposite lepton flavors is approximately 6.2%.

#### Backgrounds

We focus on the two main backgrounds to our analysis [29], *i.e.*  $t\bar{t}$ -jets and  $Zjj$  production, where the  $Z$  boson decays to taus. We generate our CKKW-matched [55] event samples with SHERPA [56]. We again obtain NLO QCD normalizations of the  $Zjj$  sample from a combination of MCFM and VBFNLO for the QCD and EW production modes, respectively, and find  $\sigma(Z \rightarrow \tau^+ \tau^-) = 0.23$  pb. For the  $t\bar{t}$  sample we extract the NNLO-inclusive  $t\bar{t}$   $K$  factor from the cross section  $\sigma_{t\bar{t}}^{\text{NNLO}} = 918$  pb [33] in comparison with the cross section by SHERPA after generator-level cuts  $\sigma_{t\bar{t}} = 888.27$  fb, which already requires the tau leptons to reconstruct  $m_H = 125$  GeV within 50 GeV.

#### B. Selection Cuts and Analysis Strategy

Our event selection follows closely the parton-level analysis of Ref. [29]. We reconstruct jets with the anti- $k_T$  jet algorithm [57] with parameter  $D = 0.4$  as implemented in FASTJET [58]. We additionally impose typical weak boson fusion cuts to suppress the background to a manageable level. More specifically, we require at least two jets with

$$p_{T,j} \geq 40 \text{ GeV}, \text{ and } |y_j| \leq 4.5, \quad (6a)$$

and the two hardest (‘‘tagging’’) jets in the event are required to have a large invariant mass

$$m_{jj} = \sqrt{(p_{j,1} + p_{j,2})^2} \geq 600 \text{ GeV}. \quad (6b)$$

After these cuts the signal is still dominated by the  $t\bar{t}$ -jets background. This background, however, can be efficiently suppressed with a  $b$  veto from the top decay.

The reconstructed taus need to be hard and central to guarantee a good reconstruction efficiency

$$p_{T,\tau} \geq 20 \text{ GeV}, \text{ and } |y_\tau| \leq 2.5. \quad (7a)$$

	$t\bar{t}$ jets $\sigma$ [fb]	Z+2 jets $\sigma$ [fb]	H+2 jets $\sigma$ [fb]	A+2 jets $\sigma$ [fb]
$p_{T,j} \geq 40$ GeV, $ y_j  \leq 4.5$ , $n_j \geq 2$	2132.46	8.52	6.21	4.12
$p_{T,\tau} \geq 20$ GeV, $ \eta_\tau  \leq 2.5$ , $n_\tau = 2$				
$m_{jj} \geq 600$ GeV	145.68	3.98	4.12	1.87
$ m_{\tau\tau} - m_H  < 20$ GeV, $ y_H  \leq 2.5$	99.86	2.29	3.99	1.82
$\exists j_a, j_b : y_{j_a} < y_h < y_{j_b}$	88.33	1.65	3.81	1.59
$b$ -veto	5.10	1.65	3.81	1.59

TABLE I: Cut flow of the analysis as described in Sec. III B. For Z+2 jets, H+2 jets and A+2 jets we normalize to their NLO QCD cross section. The  $t\bar{t}$  production cross section we normalize to the NNLO QCD cross section given in [33]. We neglect tau reconstruction efficiencies throughout. For the  $b$ -veto we assume a flat efficiency analogous to [29].

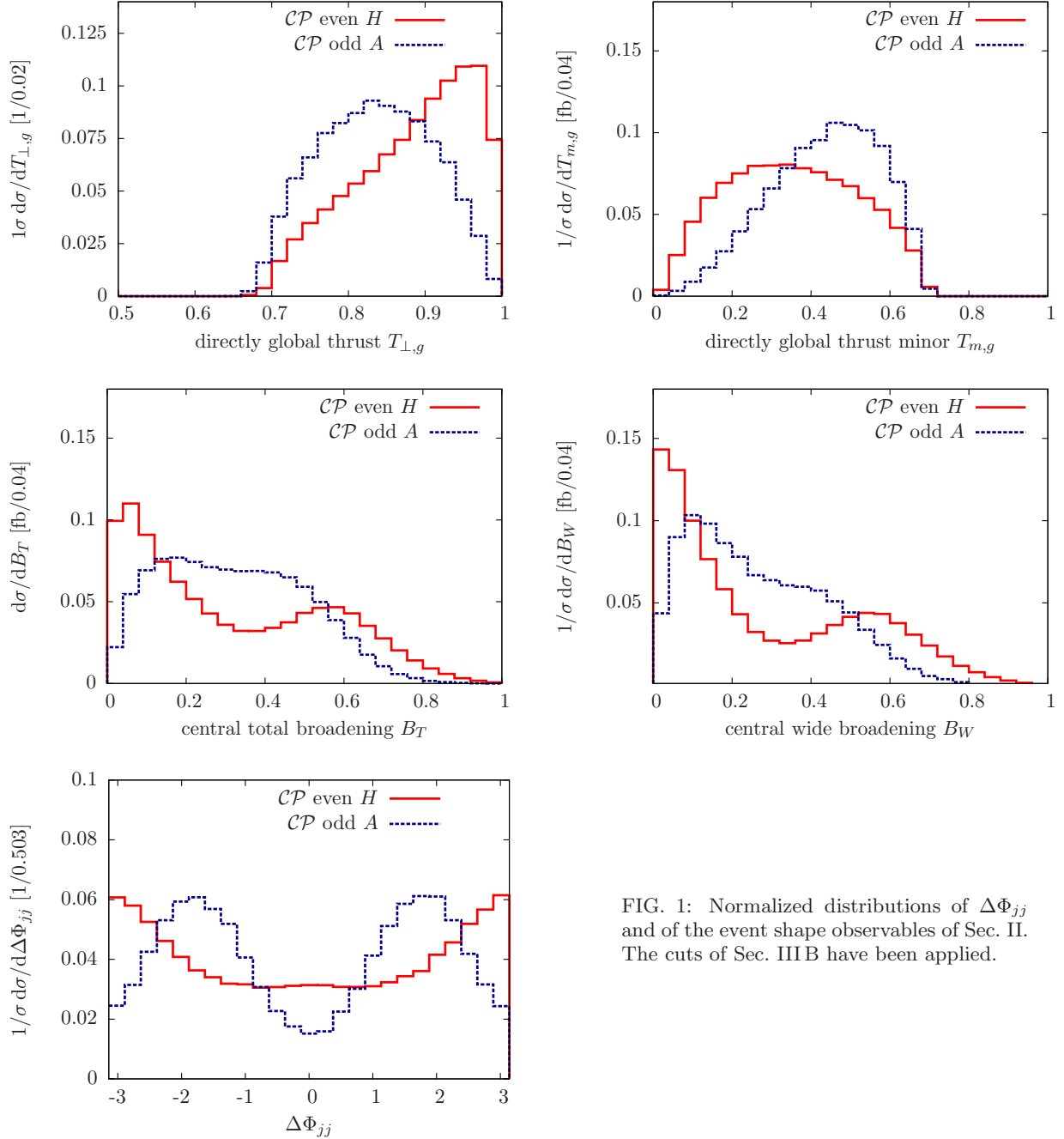


FIG. 1: Normalized distributions of  $\Delta\Phi_{jj}$  and of the event shape observables of Sec. II. The cuts of Sec. III B have been applied.

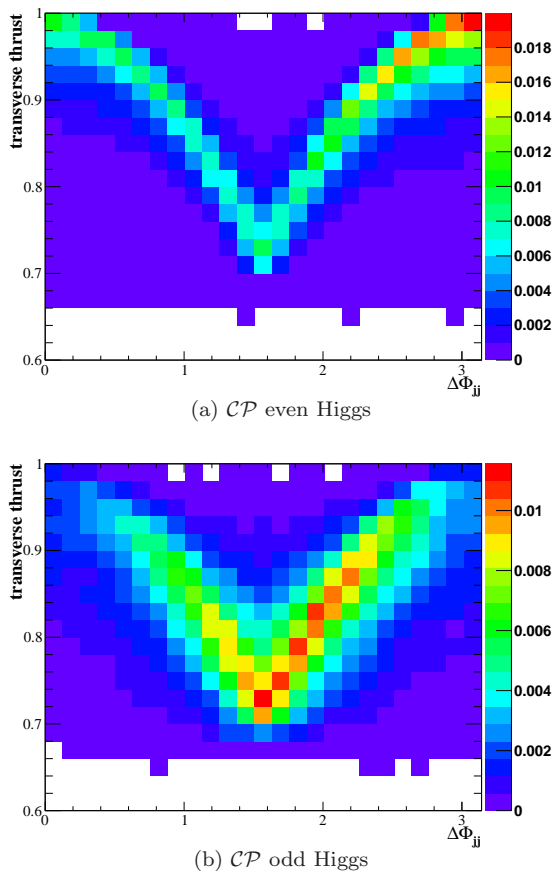


FIG. 2: Correlation of the thrust event shape with  $\Delta\Phi_{jj}$  angle as defined in Eq. (4) in terms of the 2d differential probability distribution  $1/\sigma d^2\sigma/(d\Delta\Phi_{jj} dT_{\perp,g})$

As already mentioned we limit ourselves to the clean purely leptonic ditau final state in this paper. It is however worth mentioning, that the tau reconstruction algorithms show very good reconstruction efficiencies also for (semi)hadronic decays [38, 59, 60], so that there is good reason to believe that our results can be significantly improved in a more realistic analysis.

The Higgs decay products are required to reconstruct the Higgs mass within a 40 GeV window,

$$|m_{\tau\tau} - m_H| < 20 \text{ GeV}, \quad (7b)$$

and the Higgs has to fall between two reconstructed jets,

$$\exists j_a, j_b : y_{j_a} < y_h < y_{j_b}. \quad (7c)$$

If an event passes the above selection criteria, we isolate the Higgs decay products from the event and feed all remaining final state particles with  $|\eta_i| \leq 4.5$  and  $p_{T,i} \geq 1 \text{ GeV}$  into the computation of the event shape observables discussed in the previous section. We therefore implicitly assume that the resonance has already been established and that the  $\tau$  reconstruction is efficient enough to avoid a large pollution from mistags and/or fakes. A cut-flow of the analysis steps (6)-(7) is listed in Tab. I.

Note that there is good agreement with the results of Ref. [29]. Note also that the specific selection criteria that are necessary to reduce the backgrounds can complicate the resummation of the event shapes. In particular the invariant mass cuts introduce additional scales to the problem and will have an impact in the reduction on the theoretical uncertainties.

In order to study the sensitivity of these observables without introducing a bias, we do not impose a central jet veto [19, 29, 61, 62]. In Ref. [63] it was shown that different cut efficiencies of jet vetos for WBF and GF contributions can be used to separate WBF from GF. Therefore, jet vetos in fact provide an “orthogonal” strategy to ours. Given that systematic and theoretical uncertainties of both strategies are different, a comparison or a combination of both strategies can help to reduce systematics in separating GF from WBF. This can eventually lead to smaller uncertainties in the extraction of the Higgs couplings along the lines of Eq. (1).

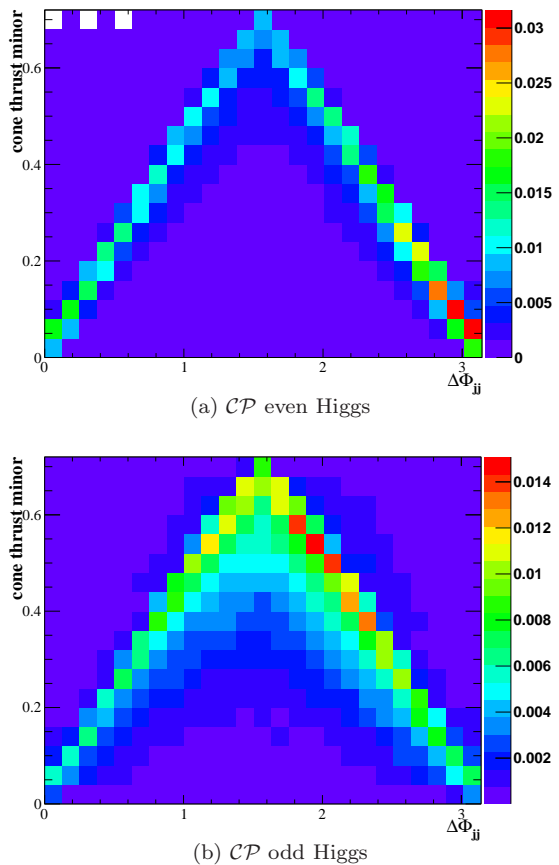


FIG. 3: Correlation of the cone thrust minor event shape with  $\Delta\Phi_{jj}$  angle as defined in Eq. (4) in terms of the 2d differential probability distribution  $1/\sigma d^2\sigma/(d\Delta\Phi_{jj} dT_{C,m})$

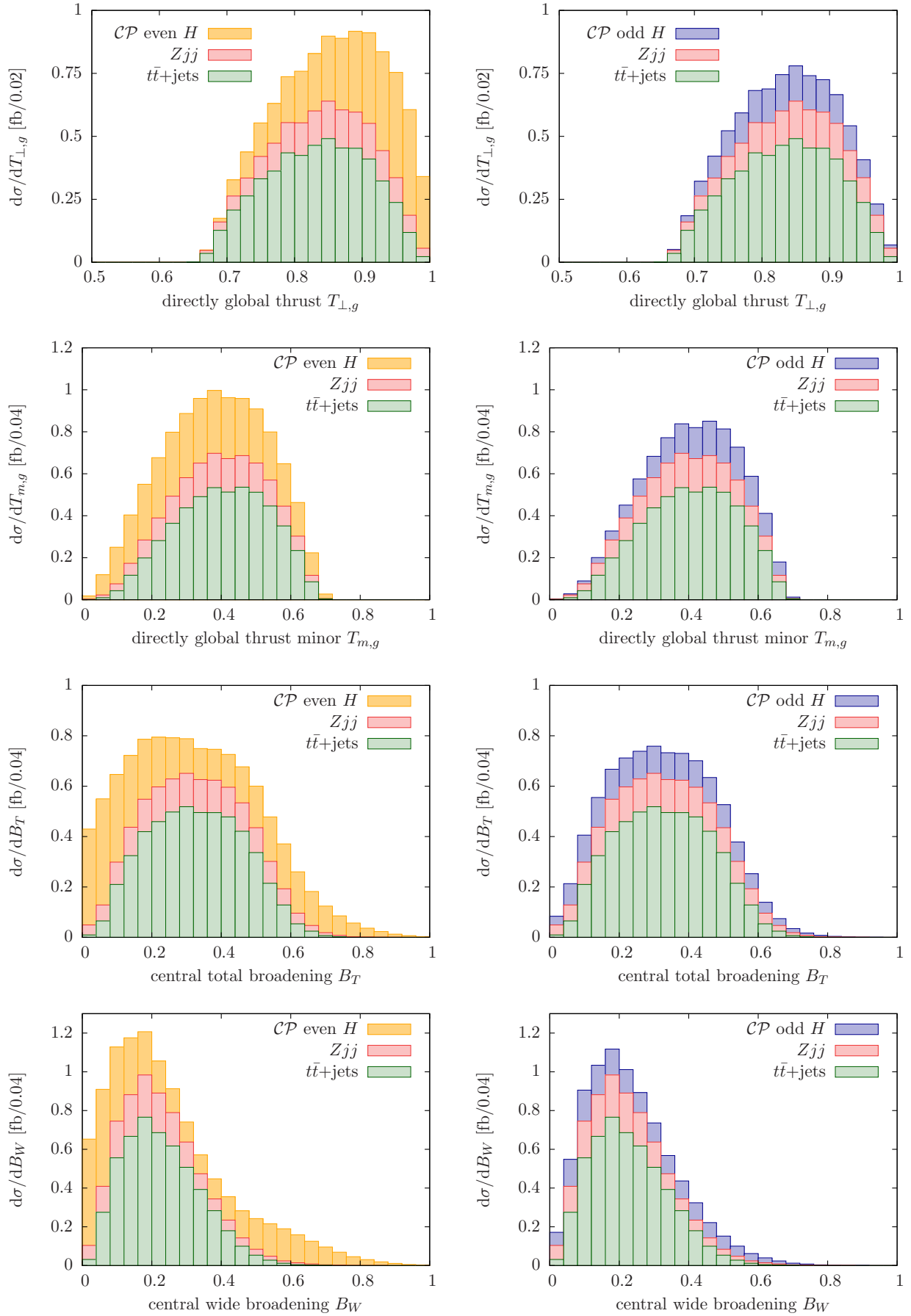


FIG. 4: Distributions of the event shape observables of Sec. II including the background after the cuts of Sec. III B.

## IV. RESULTS

### A. $\mathcal{CP}$ even vs. $\mathcal{CP}$ odd

We are now ready to study the sensitivity of the shape observables of Sec. II quantitatively. Imposing the selection cuts of the previous section, we show normalized signal distributions in Fig. 1 for the  $\mathcal{CP}$  even and odd Higgs cases. As done in Refs. [35, 37, 64] we consider  $\Delta\Phi_{jj} \in [-\pi, \pi]$ .

Fig. 1 reveals a substantial dependence on the  $\mathcal{CP}$  quantum numbers of the Higgs and the sensitivity in the azimuthal angle correlation carries over to the event shapes. This is evident when comparing to, *e.g.*, thrust, Eq. (2): a  $\mathcal{CP}$  even  $Hjj$  event has tagging jets which are preferably back-to-back. Given that the tagging jets are by construction the leading jets in the event, we observe a more pencil-like structure for the thrust observable in  $Hjj$  than we see in the  $\mathcal{CP}$  odd  $Ajj$  case. In this context, the thrust- $\Delta\Phi_{jj}$  correlation is particularly interesting, Fig. 2. Indeed, thrust and  $\Delta\Phi_{jj}$  are fairly correlated as expected after the above points. This also means that it should be possible to carry over theoretical and experimental improvements of either observable to the other one.

Another way to understand the special relation of thrust and  $\Delta\Phi_{jj}$  from a different vantage point is by investigating the jet emission pattern of Higgs+2 jets events. Due to the observed Poisson-like scaling pattern in the exclusive number of central non-tagging jets in Higgs+2 jets events once the cuts of Sec. III B are applied [19, 29, 61, 62, 65], the two-jet topology plays a special role. The two jets recoiling against the Higgs therefore largely determine the orientation of the thrust axis, and, given that both observables are defined in the beam-transverse plane, we observe a direct connection of thrust with  $\Delta\Phi_{jj}$ . This, however, is affected and washed out by soft radiation (non-resolved jets) included in the first observable. Suppressing the latter by admitting a more accentuated role to the two tagging jets, when turning to, *e.g.*, cone thrust minor, we see a more direct correlation with  $\Delta\Phi_{jj}$ , Fig. 3.

Fig. 1 gives, of course, a wrong impression of the eventual discriminative power as the normalization relative to the background and the backgrounds' shape are not included. Fig. 4 draws a more realistic picture by comparing the differential cross sections of the  $Ajj$ +background and the  $Hjj$ +background. In particular, the background mimics the  $\Delta\Phi_{jj}$  distribution of the  $\mathcal{CP}$  even  $Hjj$  events and most of the discriminating power comes from a critical signal-to-background ratio  $S/B$ . Systematic uncertainties can easily wash out the small excess around  $|\Delta\Phi_{jj}| \simeq 2$  for  $Ajj$  production in comparison to  $Hjj$ . A more quantitative statement, however, requires a dedicated Monte Carlo analysis taking into account experimental systematics and we cannot explore this direction in our analysis *in extenso*. The broadening observ-

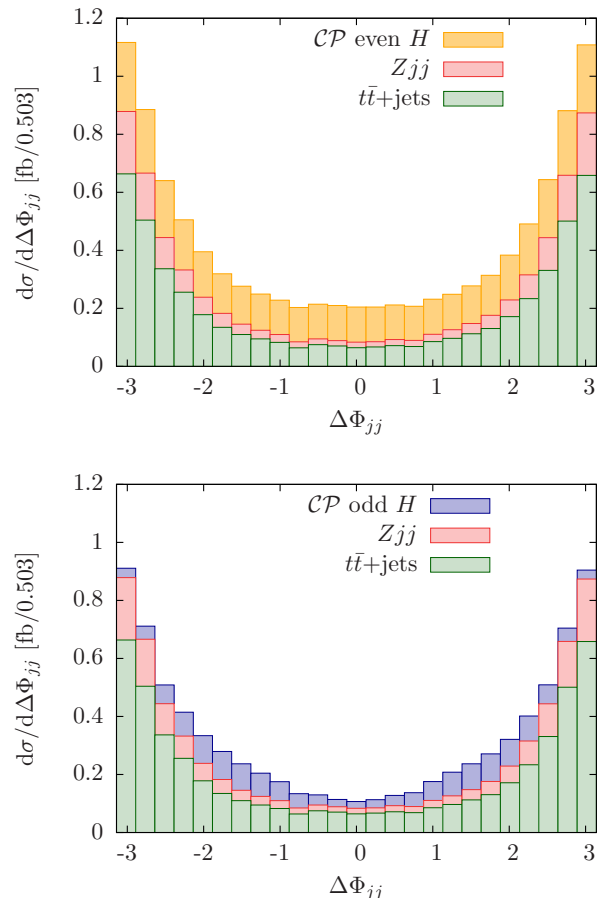


FIG. 5:  $\Delta\Phi_{jj}$  distribution including the background after the cuts of Sec. III B.

ables, on the other hand, lift the  $\Delta\Phi_{jj}$  signal-background shape-degeneracy especially in the  $\mathcal{CP}$ -even Higgs case.

We perform a binned log-likelihood hypothesis test as considered in Refs. [53, 66] to provide a statistically well-defined estimate of when we will be able to tell apart the  $\mathcal{CP}$  quantum numbers of a 125 GeV SM-like Higgs resonance. At the same time this provides a statistically well-defined picture of which observable is particularly suited for this purpose. Shape differences and different normalizations (*i.e.* due to the missing WBF component in  $Ajj$  production) are incorporated simultaneously in this approach. We comment on the discriminative power that solely arises from the different shapes later in Sec. IV B. In performing the hypothesis test we treat each individual bin in Fig. 1 as a counting experiment. Thereby we do not include any shape uncertainties, which can be different for each of the considered observables.

Hence, some words of caution are in place. On the one hand, sensitivity from *e.g.* soft radiation pattern that contributes to the overall sensitivity of the event shape observables can be weakened by pile-up (*cf.* Sec. IV D). On the other hand, increasing  $S/B$  to enhance sensitivity in  $\Delta\Phi_{jj}$  heavily relies on jet vetos which can be the-

oretically challenging. Also, the experimental resolution (which should be reflected by the binning in Figs. 4 and 5) is currently not known.

We plot the confidence levels obtained from the hypothesis test in Fig. 6 as a function of the integrated luminosity. When the confidence level (*i.e.* the probability of one hypothesis to fake the other one) is smaller than  $2.72 \cdot 10^{-7}$  one speaks of a  $5\sigma$  discrimination, implicitly assuming Gaussian-like probability density functions. We see from Fig. 6 that event shapes indeed provide a well-suited class of  $\mathcal{CP}$  discriminating observables, superseding  $\Delta\Phi_{jj}$  within the limitations of our analysis mentioned above. Fig. 6 strongly suggests that event shape observables should be added to the list of  $\mathcal{CP}$ -sensitive observables which need to be studied at the LHC to measure the Higgs'  $\mathcal{CP}$ .

### B. Higgs-lookalike $\mathcal{CP}$ odd

In fact, Fig. 6 being the result of a comparison that reflects both different shape *and* normalization of the  $A_{jj}$  and  $H_{jj}$  samples, the sensitivity that arises only due to shape differences (*cf.* Fig. 1) is not obvious. Also, from a phenomenological point of view (and this was one of our assumptions in Sec. III B), the resonance will have been discovered before we address its spin and  $\mathcal{CP}$ . Therefore the normalization of the signal will be extracted from data, and only the subsequent measurement of shapes will be used to extract information on spin and  $\mathcal{CP}$ . Hence, it is reasonable to study the discriminative power of the event shapes in comparison to  $\Delta\Phi_{jj}$  when the overall normalization after cuts of pseudoscalar and scalar are identical. This is plotted in Fig. 7. Again we see that the event shape observables are good discriminators (the comments of the previous section are applicable

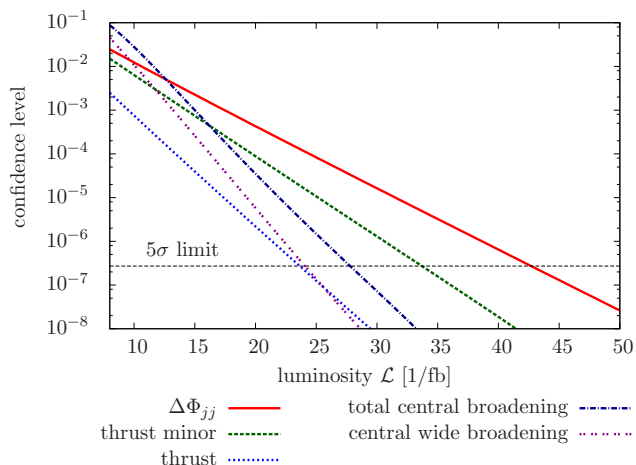


FIG. 6: Sensitivity of a binned log-likelihood shape comparison of the observables of Figs. 4 and 5. The dotted line corresponds to a  $5\sigma$  ( $2.72 \cdot 10^{-7}$  confidence level) discrimination.

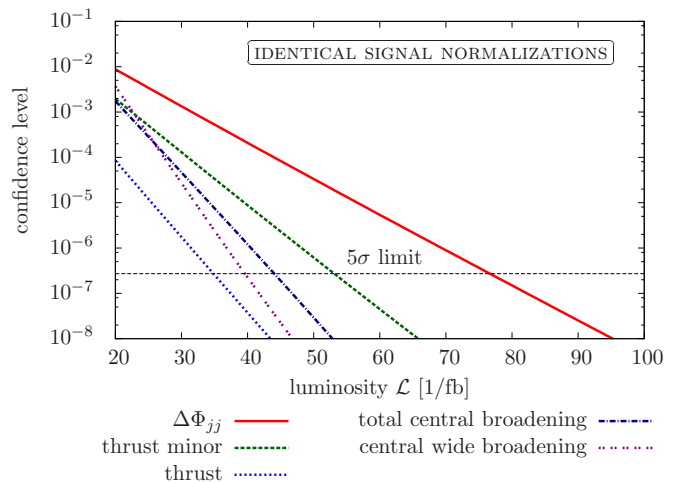


FIG. 7: Sensitivity of a binned log-likelihood shape comparison of the observables of Figs. 4 and 5 and identically chosen signal normalizations according to  $H_{jj}$ , Tab. I. The dotted line corresponds to a  $5\sigma$  ( $2.72 \cdot 10^{-7}$  confidence level) discrimination.

here as well). This also tells us that a significant share of the discriminative power found in the previous section stems from the distributions' shape. Especially the jet broadenings, which exhibit a different background distribution compared to signal for  $H_{jj}$  as opposed to  $\Delta\Phi_{jj}$ , should therefore be stressed as a discriminative observable when considering systematics.

### C. Toward discriminating gluon fusion and weak boson fusion contributions

Having established the event shape observables as  $\mathcal{CP}$ -discriminating quantities, we move on and discuss the potential of these observables to help separating WBF from GF, hence contributing to more precise determination of the Higgs couplings according to Eq. (1). We show normalized signal distributions for the individual WBF and GF contributions in Fig. 8 and we see a similar behavior as encountered in Fig. 1.

It is known that unless we include a non-renormalizable  $SU(2)_L$  axion-type dimension 5 operator  $\sim H\tilde{W}\tilde{W}$ , where  $\tilde{W}$  is the dual  $SU(2)_L$  field strength, the  $\Delta\Phi_{jj}$  distribution is almost flat in WBF [30]. While such an operator should be constrained experimentally, a sizeable  $\mathcal{CP}$ -violating coupling is not expected from a theoretical perspective. Actually, the strategy outlined in Secs. III B, IV A and IV B does not suffer from drawbacks when including explicit  $\mathcal{CP}$  violation in the gauge sector and remains applicable in a straightforward way. In fact, the relative contribution of WBF and GF to the cross section heavily influences the quantities Eqs. (2)-(5), and therefore drives the observed sensitivity in the context of  $\mathcal{CP}$  analyses, Fig. 7.

Keeping that in mind, we can use the correlations



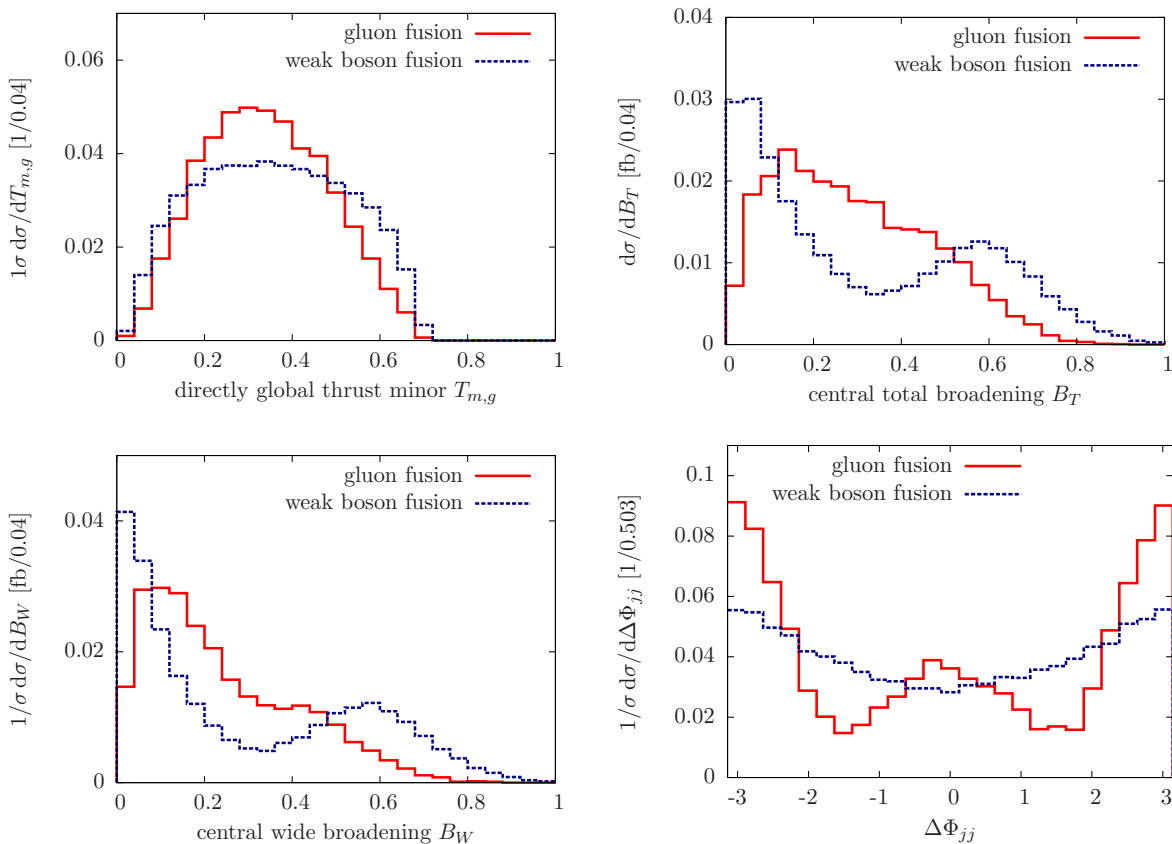


FIG. 8: Normalized distributions of  $\Delta\Phi_{jj}$  and of the event shape observables of Sec. II for separate weak boson fusion and gluon fusion contributions in case of the  $\mathcal{CP}$  even SM Higgs. The cuts of Sec. III B have been applied.

observed in Fig. 8 to separate GF from WBF. There is no meaning in performing a hypothesis test, so we limit ourselves to a discussion of the normalized distributions in the following. Forming ratios of different cut-scenarios in an ABCD-type approach, *e.g.* comparing  $0.1 \leq B_W \leq 0.5$  with the complementary region in a background-subtracted sample allows to extract the WBF and GF contributions (we stress again that interference is negligible for the chosen cuts). An assessment of the uncertainty of such an extraction, however, requires a realistic simulation, taking into account experimental systematics, and is beyond the scope of our work.

#### D. Impact of pile-up

A potential drawback, which has not been discussed in depth so far, arises from the unexpectedly high pile-up activity reported by both CMS and ATLAS for the 2011 run. Because soft tracks enter the evaluation of the event shape observables, which contain information about  $\mathcal{CP}$  or WBF vs. GF, (*cf.* Fig. 9), we expect pile-up to have an impact on the event shape phenomenology. Especially in the forward region of the detector pile-up subtraction is not available. A way to weaken the phenomenological impact of pile-up is to use jet constituents

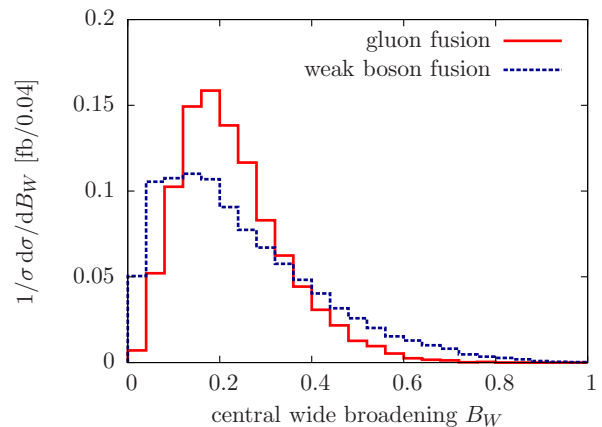


FIG. 9: Comparison of the wide broadening for the tracks which are not part of the tagging jets for WBF and GF.

as input for the even shape observables. This can distort many of the theoretical properties of event shapes (in particular resummation becomes more involved due to introduction of new scales to the problem). Hence, the potential theoretical improvements are bound to the experimental capabilities to subtract or reduce pile-up by the time the resonance is established.

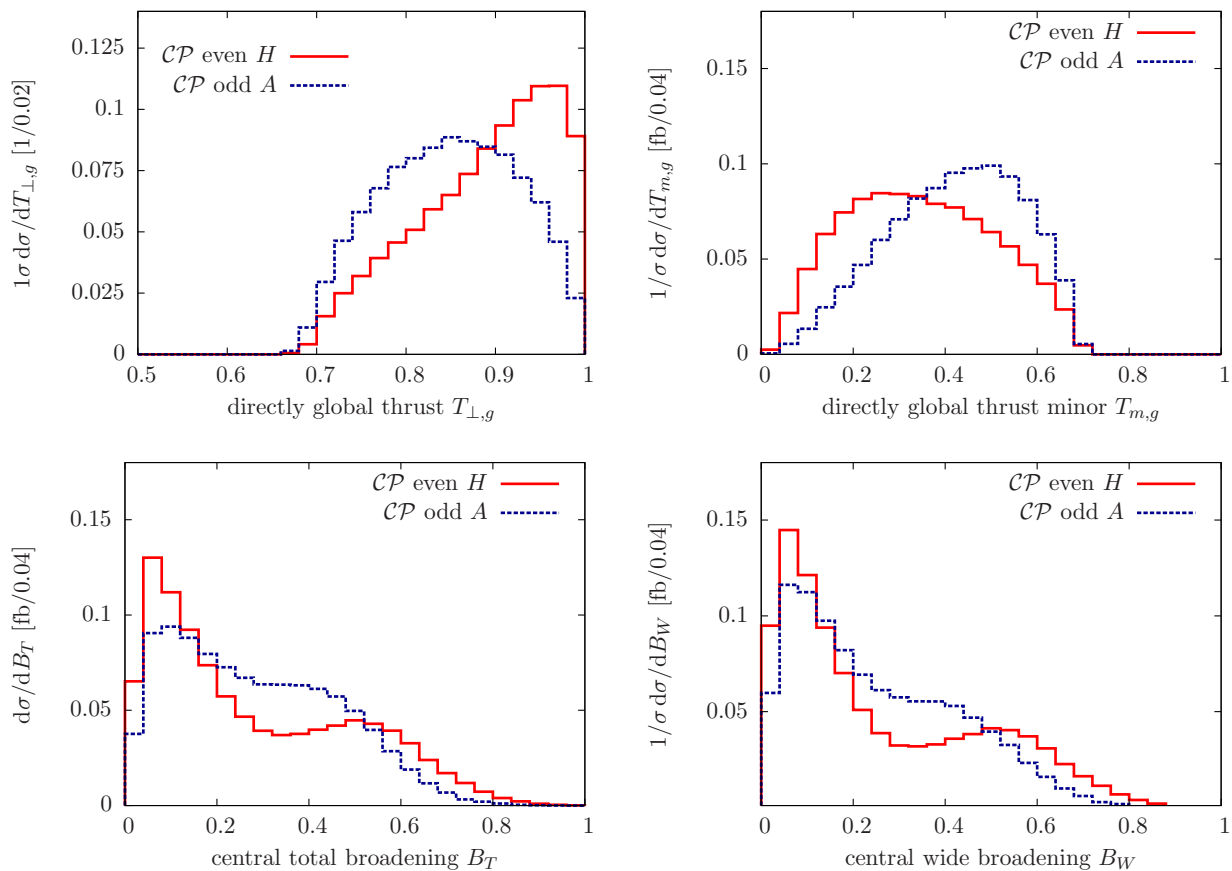


FIG. 10: Event shape observables computed from the jet constituents as outlined in Sec. IV D.

To understanding how much our sensitivity decreases by using the reconstructed jets' constituents instead of all particles, we analyze the event shapes again for a modified cut set up. We stick to the selection criteria Eqs. (6b)-(7), but modify our jet pre-selection. Again we cluster anti-kT jets with  $D = 0.4$  but consider jets

$$\begin{aligned} p_{T,j} &\geq 40 \text{ GeV}, & \text{if } 2.5 \leq |y_j| \leq 4.5, & \text{ and} \\ p_{T,j} &\geq 10 \text{ GeV}, & \text{if } |y_j| \leq 2.5. \end{aligned} \quad (6a')$$

In the central region  $|y| < 2.5$  the tracker can be used to infer the number of primary vertices of the event and here tracking serves as an efficient handle to reduce pile-up. In the forward region  $|y| > 2.5$  pile-up subtraction strategies are scarce and we rely exclusively on the hardness of the tagging jets to suppress pile-up.

Thus, we require at least three jets in the event, while the hardest two jets still have to obey  $m_{jj} > 600$  GeV, *i.e.* we try to keep as much soft central sensitivity in the first place (*cf.* Fig. 9). Instead of feeding all particles into the computation of the event shapes, we only take the constituents of the jets which pass these criteria. The signal cross sections due to the modified selection criteria decreases to 1.89 (1.35) for  $Hjj$  ( $Ajj$ ) production, yielding  $S/B \simeq 0.27$  (0.19).

The result is plotted in Fig. 10. We see that some discriminative power is lost, but the distributions are

still sensitive enough to guarantee discrimination between  $\mathcal{CP}$  even and odd (and between WBF and GF) at a however larger integrated luminosity.

## V. CONCLUSIONS AND OUTLOOK

Following the discovery of a new resonance at the LHC, the determination of its  $\mathcal{CP}$  quantum numbers and its couplings to SM fermions and gauge bosons will contribute to a more precise understanding of particle physics at a new energy frontier. Addressing these questions also poses an important test of the validity of the Standard Model after the Higgs-like resonance is established.

In this paper we have analyzed the potential of event shape observables to discriminate between different  $\mathcal{CP}$  hypotheses once a resonance is established. While more work from both theoretical and experimental sides is needed, we find excellent discrimination power for Higgs masses in the vicinity of where ATLAS and CMS have reported an excess. Sensitivity in  $\mathcal{CP}$  studies is inherited from sensitivity in telling apart weak boson fusion and gluon fusion contributions, making event shape observables natural candidates to serve this purpose in a realistic experimental analysis. The ability to sepa-

rate GF and WBF induced Higgs production will allow for an improved measurement of the Higgs couplings to fermions and electroweak gauge bosons.

We find the discriminative power of the event shapes to be fairly robust when turning to the jet level, and we therefore conclude that discriminative power should persist even under busy pile-up conditions.

We have limited our analysis to  $\sqrt{s} = 14$  TeV. Confronting data with the question for  $\mathcal{CP}$  with a statistically reasonable outcome is driven by shape analyses which typically involve  $\mathcal{O}(50 \text{ fb}^{-1})$ . It is therefore unlikely that such an analysis will be performed with the 7 TeV or 8 TeV run unless the resonance is significantly overproduced relative to the SM expectation. Nonetheless, event shape strategies can also be applied for 7 TeV or 8 TeV center-of-mass energies.

We have not exhausted the list of potentially sensitive event shape observables in our analysis. From a statistical point of view, the cross sections are large enough to eventually allow a two-dimensional analysis of observables orthogonal to the event shapes or a combination with other observables in a neural-net-based analysis. This should eventually allow to establish the  $\mathcal{CP}$  of a

125 GeV resonance shortly after its discovery.

**Acknowledgments** — We thank Andrea Banfi, Gavin Salam, and Giulia Zanderighi for making their CAESAR event shape code available to us, and we thank especially Gavin Salam for support. We thank Andy Pilkington for many helpful comments, especially concerning the separation of gluon and weak boson fusion. We also would like to thank Tilman Plehn as part of the organizing committee of the Heidelberg New Physics Forum for creating the environment where the idea for this work was born.

C.E. acknowledges funding by the Durham International Junior Research Fellowship scheme. Parts of the simulations underlying this study have been performed on bwGRiD (<http://www.bw-grid.de>), member of the German D-Grid initiative, funded by the Ministry for Education and Research (Bundesministerium für Bildung und Forschung) and the Ministry for Science, Research and Arts Baden-Württemberg (Ministerium für Wissenschaft, Forschung und Kunst Baden-Württemberg).

- 
- [1] F. Englert and R. Brout, Phys. Rev. Lett. **13** (1964) 321. P. W. Higgs, Phys. Lett. **12** (1964) 132 and Phys. Rev. Lett. **13** (1964) 508. G. S. Guralnik, C. R. Hagen and T. W. B. Kibble, Phys. Rev. Lett. **13** (1964) 585.
- [2] ATLAS Collaboration, Eur. Phys. J. C **71**, 1728 (2011).
- [3] CMS Collaboration, Phys. Lett. **B699** (2011) 25.
- [4] ATLAS and CMS collaborations, ATLAS-CONF-2011-157, CMS PAS-HIG-11-023.
- [5] ATLAS Collaboration, arXiv:1112.2577 [hep-ex], ATLAS-CONF-2011-161, ATLAS-CONF-2011-162, ATLAS-CONF-2011-163.
- [6] CMS Collaboration, CMS-PAS-HIG-11-025, CMS-PAS-HIG-11-029, CMS-PAS-HIG-11-030, CMS-PAS-HIG-11-031, CMS-PAS-HIG-11-032.
- [7] Atlas collaboration, ATLAS-CONF-2012-019. CMS collaboration, CMS-PAS-HIG-12-008.
- [8] R. Barate *et al.*, Phys. Lett. B **565** (2003) 61.
- [9] TEVNPH (Tevatron New Phenomena and Higgs Working Group) and CDF and D0 Collaborations, arXiv:1203.3774 [hep-ex].
- [10] D. Carmi, A. Falkowski, E. Kuflik and T. Volansky, arXiv:1202.3144 [hep-ph]. A. Azatov, R. Contino and J. Galloway, arXiv:1202.3415 [hep-ph]. J. R. Espinosa, C. Grojean, M. Muhlleitner and M. Trott, arXiv:1202.3697 [hep-ph].
- [11] U. Ellwanger, arXiv:1112.3548 [hep-ph]. J. F. Gunion, Y. Jiang and S. Kraml, arXiv:1201.0982 [hep-ph]. S. F. King, M. Muhlleitner and R. Nevzorov, arXiv:1201.2671 [hep-ph]. D. A. Vasquez, G. Belanger, C. Boehm, J. Da Silva, P. Richardson and C. Wymant, arXiv:1203.3446 [hep-ph].
- [12] A. Djouadi, O. Lebedev, Y. Mambrini and J. Quevillon, Phys. Lett. B **709** (2012) 65 X.-G. He, B. Ren and J. Tandeau, arXiv:1112.6364 [hep-ph].
- [13] F. Goertz, U. Haisch and M. Neubert, arXiv:1112.5099 [hep-ph]. G. Guo, B. Ren and X.-G. He, arXiv:1112.3188 [hep-ph]. C.-F. Chang, K. Cheung, Y.-C. Lin and T.-C. Yuan, arXiv:1202.0054 [hep-ph]. B. Grzadkowski and J. F. Gunion, arXiv:1202.5017 [hep-ph].
- [14] P. P. Giardino, K. Kannike, M. Raidal and A. Strumia, arXiv:1203.4254 [hep-ph].
- [15] L.F. Landau, Dok. Akad. Nauk USSR **60** (1948) 207. C.N. Yang, Phys. Rev. **77** (1950) 242.
- [16] J. Ellis and D. S. Hwang, arXiv:1202.6660 [hep-ph].
- [17] H. M. Georgi, S. L. Glashow, M. E. Machacek and D. V. Nanopoulos, Phys. Rev. Lett. **40** (1978) 692D; A. Djouadi, M. Spira and P. M. Zerwas, Phys. Lett. B **264** (1991) 440; S. Dawson, Nucl. Phys. B **359**, 283 (1991); M. Spira, A. Djouadi, D. Graudenz and P. M. Zerwas, Nucl. Phys. B **453** (1995) 17; R. V. Harlander and W. B. Kilgore, Phys. Rev. Lett. **88**, 201801 (2002); S. Moch and A. Vogt, Phys. Lett. B **631**, 48 (2005).
- [18] N. Kauer, T. Plehn, D. L. Rainwater and D. Zeppenfeld, Phys. Lett. B **503**, 113 (2001).
- [19] D. L. Rainwater, D. Zeppenfeld and K. Hagiwara, Phys. Rev. D **59** (1998) 014037.
- [20] D. Zeppenfeld, R. Kinnunen, A. Nikitenko and E. Richter-Was, Phys. Rev. D **62** (2000) 013009. M. Duhrssen, ATL-PHYS-2003-030, available from <http://cdsweb.cern.ch>. M. Duhrssen, S. Heinemeyer, H. Logan, D. Rainwater, G. Weiglein and D. Zeppenfeld, Phys. Rev. D **70** (2004) 113009. R. Lafaye, T. Plehn, M. Rauch, D. Zerwas and M. Duhrssen, JHEP **0908**, 009 (2009). M. Rauch, arXiv:1110.1196 [hep-ph].
- [21] J. Bagger, V. D. Barger, K.-m. Cheung, J. F. Gunion, T. Han, G. A. Ladinsky, R. Rosenfeld and C.-P. Yuan, Phys. Rev. D **52** (1995) 3878 C. Englert,

- B. Jager, M. Worek and D. Zeppenfeld, Phys. Rev. D **80** (2009) 035027. A. Ballestrero, D. Buarque Franzosi, L. Oggero and E. Maina, arXiv:1112.1171 [hep-ph]. P. Borel, R. Franceschini, R. Rattazzi and A. Wulzer, arXiv:1202.1904 [hep-ph]. K. Doroba, J. Kalinowski, J. Kuczmarski, S. Pokorski, J. Rosiek, M. Szleper and S. Tkaczyk, arXiv:1201.2768 [hep-ph].
- [22] S. Dittmaier *et al.* [LHC Higgs Cross Section Working Group Collaboration], arXiv:1101.0593 [hep-ph].
- [23] V. Del Duca, W. Kilgore, C. Oleari, C. R. Schmidt and D. Zeppenfeld, Phys. Rev. D **67**, 073003 (2003). F. Campanario, M. Kubocz and D. Zeppenfeld, Phys. Rev. D **84** (2011) 095025.
- [24] S. Y. Choi, D. J. Miller, M. M. Muhlleitner and P. M. Zerwas, Phys. Lett. B **553**, 61 (2003). C. P. Buszello, I. Fleck, P. Marquard and J. J. van der Bij, Eur. Phys. J. C **32** (2004) 209.
- [25] A. Bredenstein, A. Denner, S. Dittmaier and M. M. Weber, Phys. Rev. D **74** (2006) 013004. Q. H. Cao, C. B. Jackson, W. Y. Keung, I. Low and J. Shu, Phys. Rev. D **81** (2010) 015010.
- [26] N. Cabibbo and A. Maksymowicz, Phys. Rev. **137**, B438 (1965) [Erratum-ibid. **168**, 1926 (1968)].
- [27] T. L. Trueman, Phys. Rev. D **18** (1978) 3423. J. R. Dell'Aquila and C. A. Nelson, Phys. Rev. D **33** (1986) 80.
- [28] J. C. Collins and D. E. Soper, Phys. Rev. D **16** (1977) 2219.
- [29] T. Plehn, D. L. Rainwater and D. Zeppenfeld, Phys. Rev. D **61** (2000) 093005.
- [30] T. Plehn, D. L. Rainwater and D. Zeppenfeld, Phys. Rev. Lett. **88** (2002) 051801.
- [31] T. Figy, C. Oleari and D. Zeppenfeld, Phys. Rev. D **68**, 073005 (2003). T. Figy and D. Zeppenfeld, Phys. Lett. B **591**, 297 (2004). V. Del Duca, G. Klamke, D. Zeppenfeld, M. L. Mangano, M. Moretti, F. Piccinini, R. Pittau and A. D. Polosa, JHEP **0610** (2006) 016. J. M. Campbell, R. K. Ellis and G. Zanderighi, JHEP **0610** (2006) 028.
- [32] P. Nason, S. Dawson and R. K. Ellis, Nucl. Phys. B **327**, 49 (1989) [Erratum -ibid. B **335**, 260 (1990)]. W. Beenakker, W.L. van Neerven, R. Menge, G.A. Schuler and J. Smith, Nucl. Phys. B **351**, 507 (1991). M. L. Mangano, P. Nason and G. Ridolfi, Nucl. Phys. B **373**, 295 (1992). S. Frixione, M. L. Mangano, P. Nason and G. Ridolfi, Phys. Lett. B **351**, 555 (1995).
- [33] S. Moch and P. Uwer, Nucl. Phys. Proc. Suppl. **183** (2008) 75.
- [34] J. M. Campbell, R. K. Ellis, Phys. Rev. D **65** (2002) 113007. C. Oleari and D. Zeppenfeld, Phys. Rev. D **69** (2004) 093004.
- [35] J. R. Andersen, K. Arnold and D. Zeppenfeld, JHEP **1006**, 091 (2010).
- [36] J. R. Andersen and C. D. White, Phys. Rev. D **78** (2008) 051501. J. R. Andersen, V. Del Duca and C. D. White, JHEP **0902** (2009) 015. J. R. Andersen and J. M. Smillie, JHEP **1001**, 039 (2010). J. R. Andersen and J. M. Smillie, Phys. Rev. D **81**, 114021 (2010).
- [37] G. Klamke and D. Zeppenfeld, JHEP **0704** (2007) 052.
- [38] CMS Collaboration, arXiv:1202.4083 [hep-ex].
- [39] A. Banfi, G. P. Salam and G. Zanderighi, JHEP **1006** (2010) 038.
- [40] M. Dasgupta and G. P. Salam, JHEP **0208** (2002) 032 [hep-ph/0208073].
- [41] A. Banfi, G. P. Salam and G. Zanderighi, JHEP **0201** (2002) 018. A. Banfi, G. P. Salam and G. Zanderighi, JHEP **0408** (2004) 062.
- [42] A. Heister *et al.* [ALEPH Collaboration], Eur. Phys. J. C **35**, 457 (2004). J. Abdallah *et al.* [DELPHI Collaboration], Eur. Phys. J. C **37** (2004) 1. P. Achard *et al.* [L3 Collaboration], Phys. Rept. **399** (2004) 71.
- [43] A. Gehrmann-De Ridder, T. Gehrmann, E. W. N. Glover and G. Heinrich, Phys. Rev. Lett. **99** (2007) 132002. T. Becher and M. D. Schwartz, JHEP **0807** (2008) 034.
- [44] S. Brandt, C. Peyrou, R. Sosnowski and A. Wroblewski, Phys. Lett. **12**, 57 (1964). E. Fahri, Phys. Rev. Lett. **39**, (1977) 1587.
- [45] S. Catani, Y. L. Dokshitzer, M. H. Seymour, and B. R. Webber, Nucl. Phys. B **406** (1993), 187, S. D. Ellis and D. E. Soper, Phys. Rev. D **48** (1993) 3160.
- [46] S. Catani, G. Turnock and B. R. Webber, Phys. Lett. B **295** (1992) 269. Y. L. Dokshitzer, A. Lucenti, G. Marchesini and G. P. Salam, JHEP **9801** (1998) 011.
- [47] M. L. Mangano, M. Moretti, F. Piccinini and M. Trecani, JHEP **0701** (2007) 013.
- [48] J. Alwall *et al.*, JHEP **0709**, 028 (2007).
- [49] T. Sjostrand, S. Mrenna and P. Z. Skands, JHEP **0605**, 026 (2006).
- [50] J. M. Campbell and R. K. Ellis, Nucl. Phys. Proc. Suppl. **205-206** (2010) 10. R. K. Ellis, Nucl. Phys. Proc. Suppl. **160**, 170 (2006).
- [51] K. Arnold, M. Bahr, G. Bozzi, F. Campanario, C. Englert, T. Figy, N. Greiner and C. Hackstein *et al.*, Comput. Phys. Commun. **180** (2009) 1661, arXiv:1107.4038 [hep-ph].
- [52] A. Bredenstein, K. Hagiwara and B. Jager, Phys. Rev. D **77** (2008) 073004.
- [53] A. De Rujula, J. Lykken, M. Pierini, C. Rogan and M. Spiropulu, Phys. Rev. D **82** (2010) 013003.
- [54] C. Englert, C. Hackstein and M. Spannowsky, Phys. Rev. D **82** (2010) 114024
- [55] S. Catani, F. Krauss, R. Kuhn and B. R. Webber, JHEP **0111** (2001) 063.
- [56] T. Gleisberg, S. Hoeche, F. Krauss, M. Schonherr, S. Schumann, F. Siegert and J. Winter, JHEP **0902** (2009) 007. S. Schumann, F. Krauss, JHEP **0803** (2008) 038. T. Gleisberg and S. Hoeche, JHEP **0812** (2008) 039. S. Hoeche, F. Krauss, S. Schumann, F. Siegert, JHEP **0905** (2009) 053.
- [57] M. Cacciari, G. P. Salam and G. Soyez, JHEP **0804** (2008) 063.
- [58] M. Cacciari, G. P. Salam and G. Soyez, arXiv:1111.6097 [hep-ph].
- [59] M. Heldmann, D. Cavalli, ATL-PHYS-PUB-2006-008, ATL-COM-PHYS-2006-010.
- [60] CMS Collaboration, CMS-PAS-TAU-11-001, 2011.
- [61] U. Baur and E. W. N. Glover, Phys. Lett. B **252** (1990) 683. V. D. Barger, K. -m. Cheung, T. Han and D. Zeppenfeld, Phys. Rev. D **44** (1991) 2701 [Erratum-ibid. D **48** (1993) 5444]. D. L. Rainwater, R. Szalapski and D. Zeppenfeld, Phys. Rev. D **54** (1996) 6680.
- [62] E. Gerwick, T. Plehn and S. Schumann, Phys. Rev. Lett. **108** (2012) 032003.
- [63] B. E. Cox, J. R. Forshaw and A. D. Pilkington, Phys. Lett. B **696** (2011) 87. S. Ask, J. H. Collins, J. R. Forshaw, K. Joshi and A. D. Pilkington, JHEP **1201** (2012) 018.
- [64] V. Hankele, G. Klamke, D. Zeppenfeld and T. Figy, Phys. Rev. D **74** (2006) 095001.

- [65] C. Englert, T. Plehn, P. Schichtel and S. Schumann, JHEP **1202** (2012) 030.
- [66] T. Junk, Nucl. Instrum. Meth. A **434** (1999) 435. T. Junk, CDF Note 8128 [cdf/doc/statistics/public/8128]. T. Junk, CDF Note 7904 [cdf/doc/statistics/public/7904]. H. Hu and J. Nielsen, in 1st Workshop on Confidence Limits, CERN 2000-005 (2000).